The $Na^+(K^+)/H^+$ exchanger Nhx1 controls multivesicular body–vacuolar lysosome fusion

Mahmoud Abdul Karim and Christopher Leonard Brett*
Department of Biology, Concordia University, Montréal, QC H4R 1R6, Canada

ABSTRACT **Loss-of-function mutations in human endosomal $Na^+(K^+)/H^+$ exchangers (NHEs) NHE6 and NHE9 are implicated in neurological disorders including Christianson syndrome, autism, and attention deficit and hyperactivity disorder. These mutations disrupt retention of surface receptors within neurons and glial cells by affecting their delivery to lysosomes for degradation. However, the molecular basis of how these endosomal NHEs control endocytic trafficking is unclear. Using *Saccharomyces cerevisiae* as a model, we conducted cell-free organelle fusion assays to show that transport activity of the orthologous endosomal NHE Nhx1 is important for multivesicular body (MVB)-vacuolar lysosome fusion, the last step of endocytosis required for surface protein degradation. We find that deleting Nhx1 disrupts the fusogenicity of the MVB, not the vacuole, by targeting pH-sensitive machinery downstream of the Rab-GTPase Ypt7 needed for SNARE-mediated lipid bilayer merger. All contributing mechanisms are evolutionarily conserved offering new insight into the etiology of human disorders linked to loss of endosomal NHE function.**

Monitoring Editor
Suresh Subramani
University of California, San Diego

Received: Aug 4, 2017
Revised: Nov 7, 2017
Accepted: Nov 28, 2017

INTRODUCTION

Found in all organisms, $Na^+(K^+)/H^+$ exchangers (NHEs) are secondary active ion transporters that conduct exchange of monovalent cations for hydrogen ions across membranes and thus contribute to diverse physiology by regulating compartmental osmolytes, volume, and pH (Brett *et al.*, 2005a). Nhx1, an NHE in *Saccharomyce cerevisiae*, resides on endosomal compartments within cells (Nass and Rao, 1998; Kojima *et al.*, 2012). Originally identified as an important contributor to salt homeostasis (Nass *et al.*, 1997), Nhx1 was later discovered to play a pivotal role in membrane trafficking (Bowers *et al.*, 2000): Also called VPS44, NHX1 is one of ~60 *vps* (vacuole protein sorting) genes originally identified in series of classic genetic screens that revealed the molecular underpinnings of endocytic trafficking (Robinson *et al.*, 1988; Rothman *et al.*, 1989). A hallmark phenotype of NHX1 knockout (*nhx1*Δ) cells and other *vps* class E mutants is an aberrant, enlarged late endosomal compartment where internalized surface proteins and biosynthetic cargoes get trapped and accumulate en route to the vacuolar lysosome (Bowers *et al.*, 2000; Brett *et al.*, 2005b). Other *vps* class E mutants have since been shown to encode loss-of-function mutations in components of the endosomal sorting complex required for transport (ESCRT) machinery responsible for sorting and packaging internalized surface receptor and transporter proteins into intralumenal vesicles at the endosome (Henne *et al.*, 2011). Many rounds of ESCRT-mediated intralumenal vesicle formation produce mature multivesicular bodies (MVBs) that then fuse with lysosomes exposing protein-laden vesicles to acid hydrolases for catabolism. Because cells devoid of ESCRTs or NHX1 share many phenotypes, we originally hypothesized that deletion of NHX1 also prevented intralumenal vesicle formation. However, further studies revealed that intralumenal vesicle formation persists in *nhx1*Δ cells (Kallay *et al.*, 2011), albeit less efficiently than in wild-type (WT) cells (Mitsui *et al.*, 2011).

Based on data from phenomics screens, a new model of Nhx1 function emerged proposing that endocytic defects observed in *nhx1*Δ cells may be caused by MVB membrane fusion defects (Kallay *et al.*, 2011). Lending the greatest support to this hypothesis is the finding that Nhx1 binds Gyp6 (Ali *et al.*, 2004), a Rab-GTPase activating protein (Rab-GAP) that inactivates two Rab-GTPases thought to drive membrane fusion (Strom *et al.*, 1993; Vollmer *et al.*, 1999;

This article was published online ahead of print in MBoC in Press (http://www.molbiolcell.org/cgi/doi/10.1091/mbc.E17-08-0496) on December 6, 2017.

Author contributions: M.A.K. performed all experiments and prepared all data for publication. M.A.K. and C.L.B. conceived the project and wrote the article.

*Address correspondence to: Christopher Leonard Brett (christopher.brett@concordia.ca).

Abbreviations used: ESCRT, endosomal sorting complexes required for transport; GAP, GTPase-activating protein; HOPS, homotypic fusion and vacuole protein sorting; MVB, multivesicular body; NHE, Na^+/H^+ exchanger; SNARE, soluble NSF associated protein receptor; VPS, vacuole protein sorting; WT, wild type.

Will and Gallwitz, 2001): Ypt6, for MVB–*trans*-Golgi network (TGN) vesicle fusion (Bensen *et al.*, 2001; Luo and Gallwitz, 2003; Suda *et al.*, 2013; Brunet *et al.*, 2016), and Ypt7, for MVB–vacuolar lysosome (or vacuole) fusion (Balderhaar *et al.*, 2010, 2013; Epp *et al.*, 2011; Karim *et al.*, 2017). Knocking out GYP6 partially suppresses protein trafficking defects observed in *nhx1*Δ cells, suggesting that in the absence of NHX1, Gyp6 may inactivate these Rab-GTPases, preventing MVB membrane fusion events (Ali *et al.*, 2004). Since this discovery, Fratti and colleagues reported that deleting NHX1 partially blocks homotypic vacuole fusion, and Ypt7—the Rab-GTPases responsible for this event—is not likely targeted (Qiu and Fratti, 2010; Wickner, 2010). However, this does not explain how Nhx1 contributes to endocytosis or MVB biogenesis, as Nhx1 is not present on vacuole membranes within living cells (Nass and Rao, 1998; Kojima *et al.*, 2012), which is why it has been used as a reference protein to label endosomes in *S. cerevisiae* (e.g., Huh *et al.*, 2003). More importantly, this fusion event does not contribute to endocytosis. However, most of the machinery that underlies homotypic vacuole fusion is also thought to mediate MVB–vacuole fusion (Nickerson *et al.*, 2009; Kümmel and Ungermann, 2014; Karim *et al.*, 2017), implicating Nhx1 in this process.

Thus, when considering all published findings, we reasoned that Nhx1 may contribute to MVB–vacuole membrane fusion, the last step of the endocytic pathway. Recently, our group developed a cell-free assay to study the molecular mechanisms underlying this fusion event in *S. cerevisiae* (Karim *et al.*, 2017). Here we use it to test this hypothesis and begin to characterize how Nhx1 contributes to this process.

RESULTS AND DISCUSSION

Ionic requirements for MVB–vacuole fusion suggest dependence on Nhx1

All endosomal NHEs including Nhx1 contribute to ion gradients across endosome or MVB perimeter membranes where they export a lumenal H^+ ion (to regulate pH) in exchange for import of a cytoplasmic monovalent cation (to possibly regulate the osmotic gradient; Nass and Rao, 1998; Bowers *et al.*, 2000). As ionic and osmotic gradients are important for membrane fusion events underlying exocytosis and endocytosis as well as homotypic vacuole fusion (Heuser, 1989; Starai *et al.*, 2005; Brett and Merz, 2008; Cang *et al.*, 2015), we reasoned that Nhx1 activity may contribute to MVB–vacuole fusion. If true, then this fusion event should be dependent on pH and monovalent cation gradients. To test this hypothesis, we conducted a series of cell-free MVB-vacuole fusion assays that involve reconstitution of β-lactamase activity upon lumenal content mixing (see Karim *et al.*, 2017). Importantly, Nhx1-positive puncta, representing endosomes or MVBs, are present and found adjacent to vacuole membranes in organelle preparations freshly isolated from yeast cells expressing NHX1-GFP (Figure 1A), similar to its distribution in living cells (Nass and Rao, 1998). In addition, we observe the accumulation of Nhx1-GFP on membranes of large vacuoles over time under fusogenic conditions in vitro, suggesting that Nhx1-GFP is deposited on products of fusion between MVB perimeter and vacuole membranes. These important observations justify the use of our cell-free system to study the potential role of Nhx1 in MVB-vacuole fusion. Furthermore, they support the idea that MVB membranes undergo full fusion (i.e., completely merge)

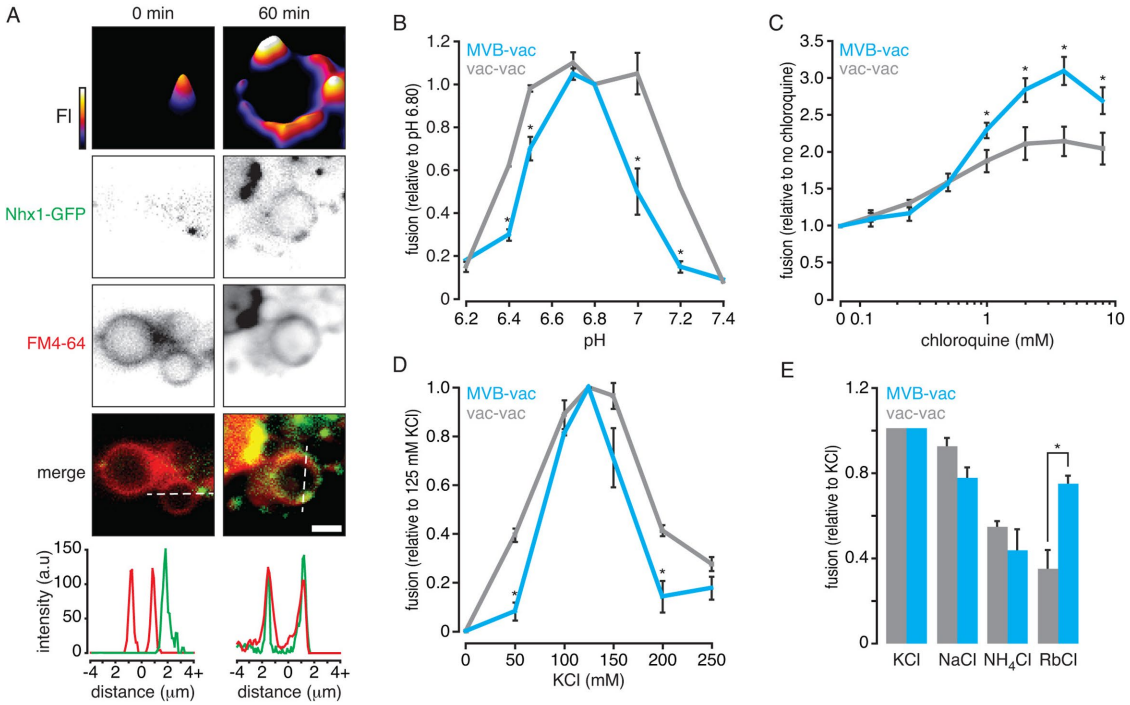

FIGURE 1: Ionic profile of MVB-vacuole fusion. (A) Fluorescence micrographs of organelles isolated from yeast cells expressing Nhx1-GFP before (0) and after (60 min) incubation under fusogenic conditions in vitro. Vacuole membranes are stained with FM4-64. Two-dimensional fluorescence intensity (FI) plots are shown for Nhx1-GFP (top). Fluorescence intensity is also plotted (bottom) for lines shown in merged images of Nhx1-GFP and FM4-64 channels. Scale bar, 2 μm. (B–E) MVB-vacuole (MVB-vac) or vacuole-vacuole (vac-vac) fusion measured in the presence of increasing pH (B), chloroquine (C), KCl (D), or when KCl was replaced with other salts (125 mM; E). All fusion reactions were incubated for 90 min at 27°C in the presence of ATP. Values were normalized to control conditions (125 mM KCl, pH 6.80, no chloroquine). Mean ± SEM ($n \geq 3$) are plotted, and p values < 0.05 (*) are shown for comparisons between MVB–vacuole and vacuole–vacuole fusion values.

with vacuole membranes to deliver lumenal contents (i.e., intralumenal vesicles) to the vacuole.

After confirming the presence of Nhx1 in our cell-free preparations, we next changed the pH of the reaction buffer to mimic changes in cytoplasmic [H^+] and examined the effect on organelle fusion in vitro (Figure 1B). Compared to homotypic vacuole fusion, MVB-vacuole fusion was more sensitive to shifts in buffer pH and a sharp peak was observed at pH 6.80, the cytoplasmic pH of yeast cells under normal growth conditions (Brett *et al.,* 2005b; Mitsui *et al.,* 2011), suggesting that small changes in cytoplasmic pH are sufficient to control MVB-vacuole fusion events. We observed a different pH profile for homotypic vacuole fusion, suggesting that the mechanism(s) conferring pH sensitivity are likely different for each fusion event.

In mammalian cells, alkalinization of the MVB lumen promotes fusion with lysosomes (Cao *et al.,* 2015) consistent with our model of endosomal NHE function, whereby Nhx1 acts as a lumenal proton leak pathway opposing the activity of the V-type H^+-ATPase (Nass and Rao, 1998). Thus, to determine whether raising lumenal pH also affects MVB–vacuole fusion in our system, we treated isolated organelles with chloroquine, a weak base that accumulates within MVBs and vacuoles to raise lumenal pH (Pearce *et al.,* 1999; Qiu and Fratti, 2010). As compared with homotypic vacuole fusion, chloroquine had a greater stimulatory effect on MVB-vacuole fusion (Figure 1C). This finding is consistent with observations in mammalian systems, as well as for homotypic vacuole fusion (Desfougères *et al.,* 2016) and confirms that this heterotypic fusion event is particularly sensitive to changes in both lumenal and cytoplasmic pH, which are regulated by Nhx1 (Brett *et al.,* 2005b; Mitsui *et al.,* 2011).

In exchange for the export of H^+, Nhx1 is thought to import a monovalent cation: K^+, Na^+, or Rb^+ and other NHEs are also known to bind and transport NH_4^+ with less affinity (Nass *et al.,* 1997; Brett *et al.,* 2005a,b). If Nhx1 activity is important for MVB-vacuole fusion, then this process should depend on the presence of these monovalent cations in the reaction buffer that mimics the cytoplasm in vitro. To test this hypothesis, we first measured organelle fusion in the presence of increasing concentrations of K^+ (as KCl), the most abundant monovalent cation in the cytoplasm and likely preferred substrate of Nhx1 (Figure 1D). As expected, MVB–vacuole fusion required KCl and peak fusion was observed near physiological concentrations (125 mM). Heterotypic fusion was less tolerant to changes in [KCl] as compared with homotypic vacuole fusion, confirming that this fusion event is sensitive to both substrates of Nhx1.

We next tested whether organelle fusion was supported by other cationic substrates by replacing K^+ with Na^+, Rb^+, or NH_4^+ (Figure 1E). Replacing K^+ with Na^+ or Rb^+ reduced heterotypic fusion by 20.4 and 22.4%, respectively, whereas replacing it with NH_4^+ diminished heterotypic fusion by 41.2%, which is consistent with the predicted relative affinities of Nhx1 for each cation (Nass and Rao, 1998; Brett *et al.,* 2005a,b). Similar results were obtained for homotypic vacuole fusion—consistent with a previous report (Starai *et al.,* 2005)—with the exception of Rb^+, which does not entirely support homotypic fusion, possibly reflecting the absence of Nhx1 or other mechanisms capable of Rb^+ transport on the vacuole. In all, these findings reveal the cationic profile of MVB–vacuole fusion, which is distinct from homotypic vacuole fusion and correlates with Nhx1 ion exchange activity.

Deleting NHX1 impairs MVB–vacuole membrane fusion

Previous studies on Nhx1 function have led to the hypothesis that deleting NHX1 blocks MVB–vacuole fusion (Bowers *et al.,* 2000; Kallay *et al.,* 2011). To test this hypothesis, we knocked out NHX1 in cells expressing fusion probes and confirmed that GFP-tagged variants of the probes properly localize to the lumen of MVB or vacuole in live cells or organelles isolated from *nhx1*Δ strains (Figure 2A). Next, we measured fusion between MVBs and vacuoles isolated from either wild-type or *nhx1*Δ cells (Figure 2B). As expected, deleting NHX1 impaired MVB–vacuole fusion, confirming that it contributes to this fusion event. However, knocking out NHX1 did not completely block this fusion event, consistent with Nhx1 possibly playing a regulatory role as opposed to being a component of the core fusion machinery which, when deleted, cause severe trafficking defects and vacuole fragmentation (i.e., *vps* class B or class C phenotypes) unlike *nhx1*Δ (a *vps* class E mutant; Robinson *et al.,* 1988; Rothman *et al.,* 1989).

Deleting NHX1 blocks delivery of some biosynthetic cargo to the vacuole (Bowers *et al.,* 2000; Brett *et al.,* 2005b). Thus, it is possible that impaired MVB-vacuole fusion may be a consequence of improper delivery of fusion proteins to vacuoles in *nhx1*Δ cells. To eliminate this possibility, we mixed organelles isolated from either wild-type or *nhx1*Δ cells expressing complementary fusion probes and measured heterotypic membrane fusion in vitro (Figure 2C). Importantly, fusion between wild-type MVBs and *nhx1*Δ vacuoles was similar to fusion between wild-type organelles, confirming that the fusion machinery was properly delivered to vacuoles in *nhx1*Δ cells, consistent with a previous report (Qiu and Fratti, 2010). However, fusion between *nhx1*Δ MVBs and wild-type vacuoles was impaired, similarly to fusion between only *nhx1*Δ organelles. This important finding indicates that the underlying fusion defect is inherent to the MVB membrane, where Nhx1 resides, not the vacuole membrane.

What prevents the MVB perimeter membrane from fusing with the vacuole membrane when NHX1 is deleted? One possibility is that the underlying fusion machinery, such as the Rab-GTPase Ypt7, its cognate multisubunit tethering complex homotypic fusion and vacuole protein sorting complex (HOPS), or SNAREs may be missing on MVB membranes in *nhx1*Δ cells. To test this hypothesis, we tagged Ypt7 or subunits of HOPS (Vps41 or Vps33) with GFP and examined their distribution within live yeast cells (Figure 2D). Ypt7-GFP, Vps41-GFP, and Vps33-GFP were present on puncta (representing MVBs) and vacuole membranes in *nhx1*Δ cells, similarly to their distributions in wild-type cells (also see Auffarth *et al.,* 2014). This finding is consistent with a previous work showing that these and other fusogenic proteins required for this fusion event (e.g., the SNAREs Vam3, Vam7, and Nyv1) are present at similar levels as wild-type organelle preparations containing MVBs and vacuoles isolated from *nhx1*Δ cells (Qiu and Fratti, 2010). To confirm that SNAREs were functional on MVBs isolated from *nhx1*Δ cells, we next stimulated fusion in vitro with the soluble Qc-SNARE rVam7 in place of ATP, which drives trans-SNARE pairing and zippering to stimulate MVB-vacuole fusion, independent of Ypt7 and HOPS function (Thorngren *et al.,* 2004). Indeed, rVam7 rescued fusion of organelles isolated from *nhx1*Δ cells (Figure 2E). In all, these findings confirm that core fusion machinery is intact on MVBs isolated from *nhx1*Δ cells.

Nhx1 does not target Ypt7 to regulate MVB-vacuole fusion

How does ion transport by Nhx1 affect the fusion machinery? It was shown previously that Nhx1 binds and inhibits Gyp6, a Rab-GTPase activating protein (Rab-GAP) that can inactivate Ypt7, the Rab-GTPase responsible for MVB–vacuole fusion (Vollmer *et al.,* 1999; Will and Gallwitz, 2001; Ali *et al.,* 2004; Brett *et al.,* 2008; Karim *et al.,* 2017). Thus, we hypothesized that in the absence of NHX1, Gyp6 should be stimulated and inactivate Ypt7 on MVB membranes to prevent MVB–vacuole fusion. To test this hypothesis, we first

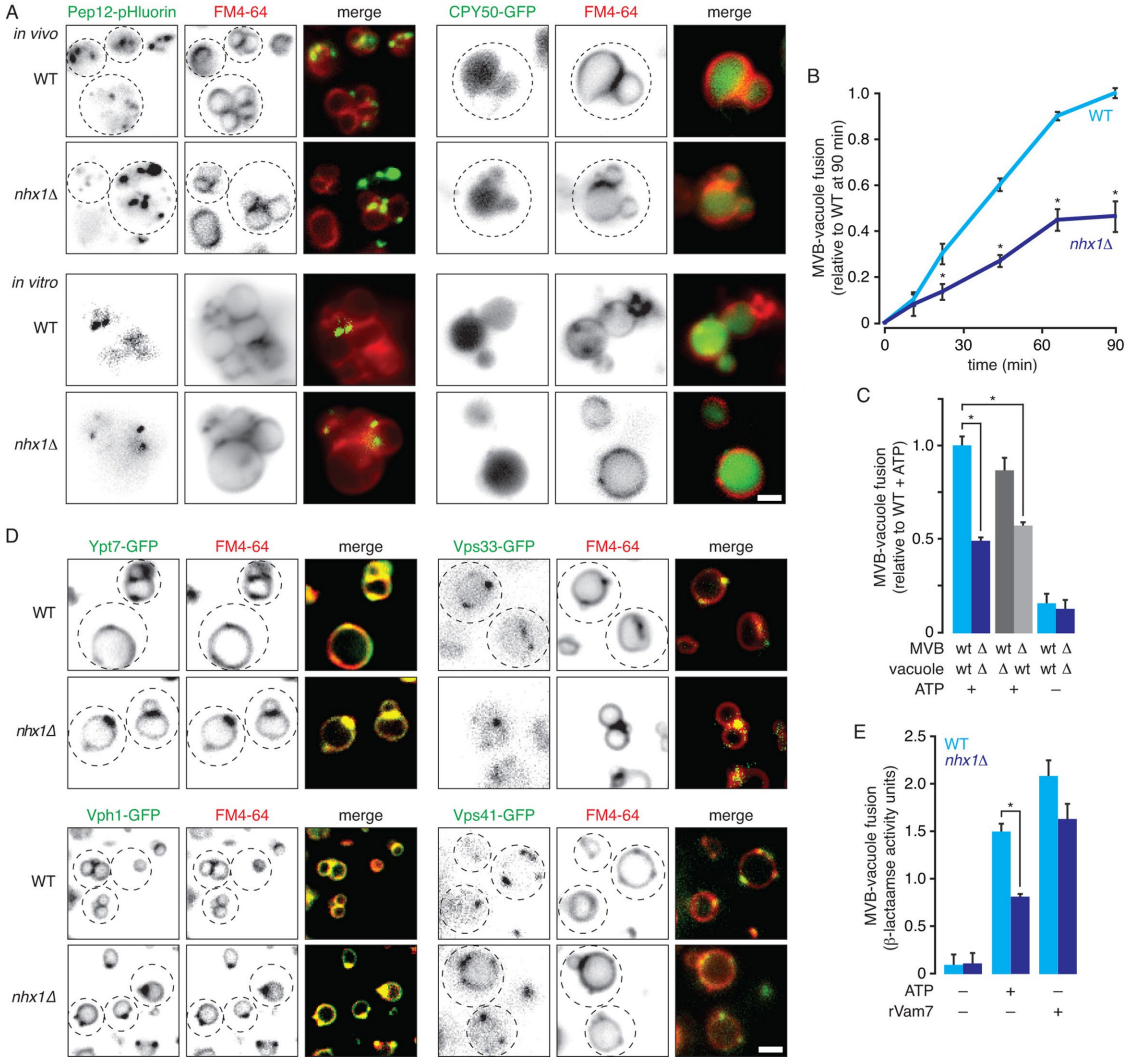

FIGURE 2: Deleting NHX1 impairs MVB–vacuole membrane fusion by targeting SNAREs. (A) Fluorescence micrographs of wild-type (WT) or *nhx1*Δ cells (top) or isolated organelles (bottom) expressing Pep12-pHluorin or CPY50-GFP. Vacuole membranes are stained with FM4-64. (B) MVB–vacuole fusion between organelles isolated from WT or *nhx1*Δ cells measured over time in the presence of ATP. (C) MVB–vacuole fusion measured after mixing organelles from WT or *nhx1*Δ (Δ) cells expressing either MVB or vacuole fusion probes. Reactions were incubated for 90 min at 27°C in the absence or presence of ATP. (D) Fluorescence micrographs of WT or nhx1Δ cells expressing Ypt7, Vph1, Vps33, or Vps41 fused to GFP. Vacuole membranes are stained with FM4-64. (E) MVB–vacuole fusion between organelles isolated from WT or *nhx1*Δ cells in the presence or absence of ATP or 100 nM rVam7. Mean ± SEM ($n \geq 3$) are plotted, and p values <0.05 (*) are shown for comparisons between wild-type and *nhx1*Δ MVB–vacuole fusion values. Dotted lines outline cell perimeter as assessed by differential interference contrast (DIC). Scale bars, 2 μm.

assessed the proportion of active Ypt7 protein present on isolated organelles by adding a purified, recombinant Gdi1, a Rab-chaperone protein (rGdi1), to isolated organelles. Gdi1 selectively binds and extracts inactive Rab from isolated membranes, allowing us to separate the pool of soluble rGdi1-bound inactive Ypt7 from membrane bound (presumably active) Ypt7 by differential centrifugation (Brett *et al.*, 2008). Compared to organelles isolated from wild-type cells, MVBs and lysosomes from *nhx1*Δ cells contained similar amounts of active Ypt7 on membranes (Figure 3A), and this pool of Ypt7 was equally susceptible to inactivation by Rab-GAP activity (by adding recombinant Gyp1-46 protein, which contains the catalytic TBC domain of the Rab-GAP Gyp1) or activation by addition of GTPγS a nonhydrolysable analog of GTP, suggesting that deleting NHX1 has no effect on Ypt7 activity.

To further test this hypothesis, we treated fusion reactions containing organelles isolated from WT or *nhx1*Δ cells with increasing concentrations of the Ypt7 inhibitors rGdi1 or rGyp1-46 (Eitzen *et al.*, 2000; Brett and Merz, 2008). We reasoned that if less active Ypt7 was present on membranes in absence of NHX1, then MVB–vacuole fusion should be more susceptible to inhibition by these proteins. However, responses to rGdi1 or rGyp1-46 were similar in the presence or absence of NHX1 (Figure 3, B and C), suggesting that loss of NHX1 does not affect the activation state of Ypt7.

These results are in stark contrast to the effect of deleting components of the ESCRT machinery (e.g., Vps27, a component of ESCRT-I; Henne *et al.*, 2011), whereby abolishing ESCRT-mediated intralumenal vesicle formation prevents proper maturation of MVBs,

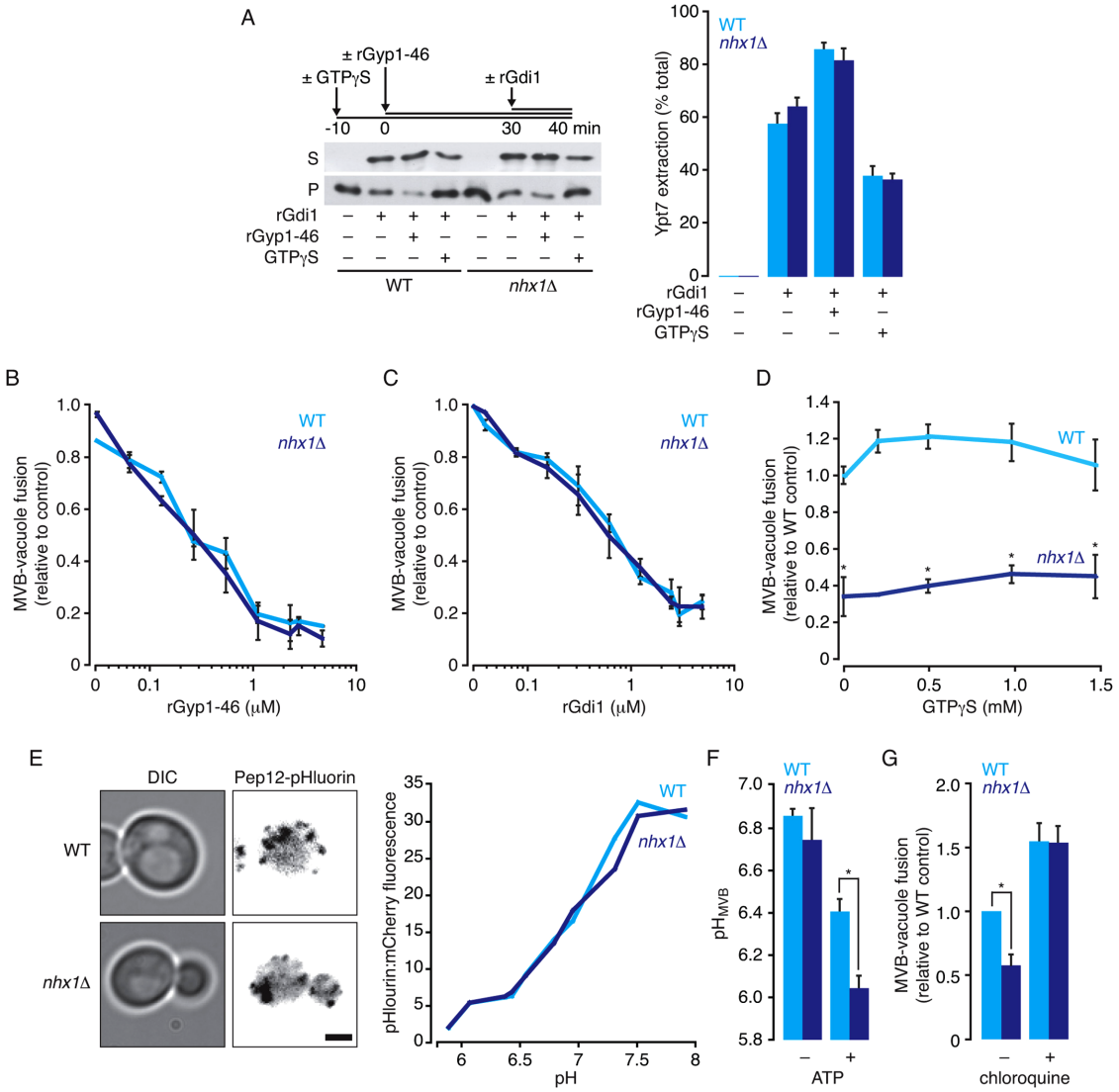

FIGURE 3: MVB–vacuole fusion defect caused by nhx1Δ is due to lumenal hyperacidification, not Rab-GTPase inactivation. (A) Organelles isolated from wild-type (WT) or *nhx1*Δ cells were incubated with ATP for 40 min with or without 10 μM rGdi1 during the last 10 min. Reactions were treated with 0.2 mM GTPγS or 5 μM rGyp1-46 where indicated. After incubation, membrane-bound (pellet, P) and soluble (supernatant, S) proteins were separated by centrifugation, and Ypt7 in each fraction was assessed by immunoblotting (left). Densitometric analysis of Ypt7 extraction (% total protein found in soluble fraction) is shown (right). (B–D) MVB–vacuole fusion between organelles isolated from WT or *nhx1*Δ cells measured in the absence or presence of increasing rGyp1-46 (B), rGdi1 (C), or GTPγS (D). Values were normalized to control conditions (no inhibitors or GTPγS). (E) pHluorin fluorescence and DIC micrographs of WT or *nhx1*Δ cells expressing Pep12-pHluorin-mCherry (left). Scale bar, 2 μm. Right, Calibration curves showing probe florescence at increasing pH values in both strains. (F) Lumenal pH of isolated MVBs from WT or *nhx1*Δ cells measured in the presence or absence ATP. (G) MVB–vacuole fusion between organelles isolated from WT or *nhx1*Δ cells measured in the absence or presence of 4 mM chloroquine. All fusion reactions were incubated for 90 min at 27°C in the presence of ATP. Means ± SEM ($n \geq 3$) are plotted, and p values < 0.05 (*) are shown for comparisons between wild-type and *nhx1*Δ MVB–vacuole fusion or pH_{MVB} values.

which in turn, blocks subsequent fusion with vacuoles presumably by disrupting a Rab conversion mechanism required for Ypt7 activation (Russell *et al.*, 2012; Karim *et al.*, 2017). In support of this model, we have previously shown that replacing wild-type YPT7 with a mutant locked in its active state (Ypt7-Q68L) rescues this fusion defect, as does addition of GTPγS to fusion reactions in vitro (which irreversibly activates Ypt7; Karim *et al.*, 2017). Although contentious (see Kallay *et al.*, 2011), Kanazawa and colleagues have proposed that knocking out NHX1 may prevent recruitment of Vps27 to endosome membranes, partially blocking ILV formation (Mitsui *et al.*, 2011). If true, then defective MVB maturation caused by deleting NHX1 should also prevent Rab conversion, and MVB–vacuole fusion should be rescued by GTPγS. However, when we tested this hypothesis, we found that addition of GTPγS did not rescue fusion between MVBs and vacuoles isolated from *nhx1*Δ cells (Figure 3D), consistent with results presented herein and previous reports (Kallay *et al.*, 2011). Thus, in all, these results suggest that Nhx1 activity does not affect Ypt7 function, unlike perturbing ESCRT function, but rather

targets another mechanism needed to promote efficient trans-SNARE pairing and zippering for MVB–vacuole fusion.

Lumenal hyperacidification correlates with a MVB–vacuole fusion defect in nhx1Δ cells

Deleting NHX1 hyperacidifies the lumen of MVBs (or endosomes) and vacuoles in living cells, and treating them with weak bases, such as chloroquine or methylamine, rescues endocytic trafficking defects (Ali *et al.,* 2004; Brett *et al.,* 2005b; Mitsui *et al.,* 2011). Specifically, they prevent accumulation of internalized surface proteins at the MVB within *nhx1*Δ cells and allow proper delivery to the vacuole lumen, where they are degraded. This observation suggests that MVB–vacuole fusion defects caused by deleting NHX1 can be overcome by the addition of weak bases. However, prior to testing this hypothesis, we first confirmed that MVBs isolated from *nhx1*Δ were indeed hyperacidic. Using an approach similar to that reported by Hiroshi Kanazawa and colleagues (Mitsui *et al.,* 2011), we measured lumenal LE pH by tagging the lumenal face of endosomal Qa-SNARE Pep12 with a pH-sensitive variant of GFP called pHluorin. After demonstrating that the probe was properly localized to MVBs and responsive to pH in our organelle preparations (Figure 3E), we confirmed that enlarged MVBs isolated from *nhx1*Δ cells were hyperacidified (Figure 3F), validating our use of this cell-free assay to study the role of Nhx1 in MVB–vacuole fusion. Importantly, we show that MVB acidification is ATP dependent, confirming that ATP is needed to drive H^+-pumping by the V-type H^+-ATPase (or V-ATPase), in support the prevailing model of MVB pH regulation that describes Nhx1 as a lumenal H^+ leak pathway that opposes V-type H^+-ATPase function (Nass and Rao, 1998).

We next determined whether addition of the weak based chloroquine rescues MVB–vacuole fusion defects caused by NHX1 deletion (Figure 3G). As predicted, chloroquine completely rescued MVB-vacuole fusion, consistent with previous reports that H^+ transport by Nhx1 is essential for delivery of internalized surface membrane proteins to vacuoles for degradation in live cells (Brett *et al.,* 2005b). Weak bases also rescue homotypic vacuole fusion defects caused by deleting NHX1 (Qiu and Fratti, 2010), suggesting the underlying mechanism may be similar.

What senses and responds to pH at MVBs to initiate fusion with vacuoles? Before we speculate, it is important to acknowledge that Nhx1 is thought to translocate H^+ from the lumen to the cytoplasm; thus, alterations in pH on either side of the MVB perimeter membrane may contribute to the fusion defect caused by deleting NHX1. On the cytoplasmic side, loss of Nhx1 activity may deplete H^+ near the outer leaflet of the MVB lipid bilayer. Data presented in Figure 1B suggest that even a small decrease in cytoplasmic [H^+] (from pH 6.8 to pH 7.2) completely blocks fusion. MVB and vacuole membrane outer leaflets are enriched with negatively charged phospholipid species, for example, phosphatidylinositide-3-phosphate and phosphatidic acid (Gillooly *et al.,* 2000; Fratti *et al.,* 2004). Many components or regulators of the fusion protein machinery are recruited to the membrane by binding these lipids, including the Ypt7 guanine exchange factor complex Mon1-Ccz1 (Lawrence *et al.,* 2014), HOPS (Stroupe *et al.,* 2006), Vac1 and Vps45 mediated by FYVE (Fab1-YOTB-Vac1-EEA1)-containing domains (Peterson *et al.,* 1999; Tall *et al.,* 1999), and Vam7 through its PX domain (Fratti and Wickner, 2007). As it has been proposed that local H^+ can protonate these lipids to modulate recruitment of the fusion protein machinery to the membrane (He *et al.,* 2009; Shin and Loewen, 2011), it is possible that deleting NHX1 perturbs lipid protonation on the cytoplasmic leaflet disrupting recruitment of fusion proteins to the MVB membrane. Although appealing, we argue that this possibility is unlikely because deleting NHX1 has no effect on pH near the cytoplasmic leaflet of the MVB membrane (Mitsui *et al.,* 2011). Furthermore, we do not observe changes in cellular distributions of GFP-labeled components of HOPS (Figure 2D), and Ypt7 can be activated in *nhx1*Δ cells, indicating that negatively charged lipids on MVB membranes continue to recruit soluble components of the fusion machinery.

Rather, we propose that the reduction in pH on the lumenal side of the MVB membrane contributes to the fusion defect in *nhx1*Δ cells. This is supported by two important observations: Fusion is rescued by adding a weak base to raise lumenal pH (Figure 3G) or by adding rVam7 to stimulate fusion in the absence of ATP, a condition that does not allow lumenal hyperacidification by the V-type H^+-ATPase in vitro (see Figure 3F). However, the molecular basis of sensing lumenal pH within organelles of the endocytic system largely remains an enigma. It has been suggested that subunits of the V-type H^+-ATPase may sense lumenal H^+ ion concentrations within the vacuole (or lysosome) to regulate fusion and other cellular roles (e.g., trigger cytoplasmic TOR [target of rapamycin] signaling in response to cellular metabolism; Maxson and Grinstein, 2014; Lim and Zoncu, 2016). Although contentious (Coonrod *et al.,* 2013), the V-type H^+-ATPase is also implicated in the homotypic vacuole fusion reaction, whereby it was proposed to mediate pore formation, a critical intermediate of the lipid bilayer fusion (Peters *et al.,* 2001). Interestingly, Vph1, the stalk domain of the V-ATPase that is exclusively found on vacuole membranes in wild-type cells, is redistributed onto enlarged MVBs when NHX1 is deleted (Bowers *et al.,* 2000). Thus, it is possible that the V-type H^+-ATPase, possibly through its interactions with SNARE proteins (Strasser *et al.,* 2011), may link Nhx1 function to MVB-vacuole fusion.

Relevance to human disease

Mutations in the human orthologues of yeast NHX1, the endosomal $Na^+(K^+)$ exchangers NHE6 and NHE9 (Brett *et al.,* 2002, 2005a; Hill *et al.,* 2006) are linked to neurological diseases such as Christianson syndrome, autism, attention deficit and hyperactivity disorder, and epilepsy (Gilfillan *et al.,* 2008; Lasky-Su *et al.,* 2008; Morrow *et al.,* 2008; Markunas *et al.,* 2010; Cardon *et al.,* 2016; Yang *et al.,* 2016). However, the etiology is not entirely understood. Given that human NHE6 or NHE9 replace some functions of Nhx1 in *S. cerevisiae* (Hill *et al.,* 2006) and that the genes encoding the machinery responsible for MVB–vacuole (or lysosome) fusion are found in all eukaryotes (Luzio *et al.,* 2010), we predict that the cellular roles of endosomal NHEs are evolutionarily conserved. Indeed, compelling work by the Morrow, Walkley, Strømme, and Orlowski groups demonstrates a strikingly similar role for mammalian NHE6 within neurons, where it seems important for endocytosis of surface TrkB/brain derived neurotropic factor receptors needed for cell signaling events underlying proper development of neural circuitry (Strømme *et al.,* 2011; Ouyang *et al.,* 2013; Deane *et al.,* 2013). Mutations in NHE6 or NHE9 are also thought to impair endocytosis in astrocytes possibly underlying cellular defects that contribute to Alzheimer's disease (Prasad and Rao, 2015) or glioblastoma (Kondapalli *et al.,* 2015). In all cases, impairment of endosomal NHE function correlates with hyperacidification of endosomes (or MVBs; Kondapalli *et al.,* 2013; Ouyang *et al.,* 2013). Thus, it is tempting to speculate that loss-of-function mutations in NHE6 or NHE9 also disrupt MVB-lysosome membrane fusion to impair endocytosis contributing to the pathogenesis of these human diseases.

MATERIALS AND METHODS

Yeast strains and reagents

For organelle content mixing assays, we used the *S. cerevisiae* strain BJ3505 [*MATα;pep4::HIS3;prbΔ1-1.6R;his3–Δ200;lys2–801;trp1-Δ101(gal3);ura3–52;gal2;can1*] transformed with expression plasmids containing the MVB fusion probe (pCB002 and pCB003) or vacuole fusion probe (pYJ406-Jun-Gs-α and pCB011; see Karim *et al.,* 2017). NHX1::GFP was knocked in or NHX1 was knocked out of BJ3505 cells using the Longtine method (Longtine *et al.,* 1998). To confirm proper fusion probe localization, WT or *nhx1*Δ BJ3505 cells were transformed with an expression plasmid containing the MVB targeting sequence (Pep12) fused to pHluorin (pCB035) or the vacuole targeting sequence (CPY50) fused to GFP (pCB044; see Karim *et al.,* 2017). Reagents were purchased from Sigma-Aldrich, Invitrogen, or BioShop Canada. Purified rabbit polyclonal antibody against Sec17 or Ypt7 were gifts from William Wickner (Dartmouth College, Hanover, NH) and Alexey Merz (University of Washington, Seattle, WA), respectively. Recombinant Gdi1 (Brett *et al.,* 2008), Gyp1-46 (the catalytic domain of the Rab-GTPase activating protein Gyp1; Eitzen *et al.,* 2000), Vam7 (Schwartz and Merz, 2009), or c-Fos (Jun and Wickner, 2007) proteins were purified as previously described. Reagents used in fusion reactions were prepared in 10 mM PIPES (2,2′-piperazine-1,4-diylbisethanesulfonic acid)-KOH, pH 6.8, and 200 mM sorbitol (PIPES–sorbitol buffer, PS).

Organelle isolation and membrane fusion

Organelles were isolated from yeast cells by the ficoll method as previously described (Karim *et al.,* 2017). To assess organelle membrane fusion, organelle content mixing was measured using a complementary split β-lactamase-based assay (see Jun and Wickner, 2007; Karim *et al.,* 2017). In brief, organelles were isolated from separate yeast strains expressing a single fusion probe targeting either the MVB or vacuole. The amount of 6 µg of organelles isolated from each complementary strain were added to 60 µl fusion reactions in standard fusion buffer (125 mM KCl, 5 mM $MgCl_2$, 10 µM coenzyme A in PS) supplemented with 11 µM recombinant c-Fos protein to reduce background caused by lysis. ATP regenerating system (1 mM ATP, 40 mM creatine phosphate, 0.5 mg/ml creatine kinase) or 100 nM recombinant Vam7 protein (and 10 µg/ml bovine serum albumin [BSA]) were added to stimulate fusion. Reactions were incubated up to 90 min at 27°C and then stopped by placing them on ice. Content mixing was quantified by measuring the rate of nitrocefin hydrolysis by reconstituted β-lactamase. A total of 58 µl of the fusion reaction was transferred into a black 96-well clear-bottom plate and mixed with 142 µl of nitrocefin developing buffer (100 mM NaPi, pH 7.0, 150 µM nitrocefin, 0.2% Triton X-100). To measure nitrocefin hydrolysis, absorbance at 492 nm was monitored at 15-s intervals for 15 min at 30°C with a Synergy H1 plate reader, a multimode spectrophotometer (Biotek, Winooski, VT). Slopes were calculated, and one fusion unit is defined as 1 nmol of hydrolyzed nitrocefin per minute from 12 µg of organelle proteins. Where indicated, purified antibodies raised against Sec17, purified recombinant Gdi1, or Gyp1-46, GTPγS, chloroquine were added to fusion reactions at concentrations indicated. In addition, pH or [KCl] of the fusion buffer was adjusted or KCl was replaced with equimolar (125 mM) NaCl, NH_4Cl, or RbCl, as indicated. Experimental results shown are calculated from greater than or equal to three biological replicates, each repeated twice (greather than or equal to six technical replicates total).

Ypt7 extraction assay

Ypt7 extraction assays were performed as previously described (Brett *et al.,* 2008). Briefly, 5× reactions containing 30 µg organelles isolated from WT or *nhx1*Δ cells were incubated at 27°C for 30 min under fusion conditions. As a positive control, 5 µM rGyp1-46 was added to promote Ypt7 inactivation and extraction; as a negative control, organelles were pretreated with 0.2 mM GTPγS for 10 min prior to incubation to promote Ypt7 activation preventing extraction. rGdi1 (10 µM) was then added, and reactions were further incubated for 10 min. Samples were then immediately centrifuged (5000 × *g*, 5 min, 4°C) to separate membrane-bound (pellet) from soluble (supernatant) Ypt7 protein. Pellets were resuspended in 100 µl 1× of reaction buffer, and 100 µl of the supernatant was mixed with 25 µl 5× Laemmli sample buffer and then boiled for 10 min. One-tenth of the total fraction volume was analyzed by immunoblotting using a purified rabbit antibody-raised against Ypt7 (see Karim *et al.,* 2017). Western blots shown are the best representatives of three biological replicates, each repeated twice (six technical replicates total).

MVB pH measurement

On the basis of a previous method used to measure lumenal MVB pH (Mitsui *et al.,* 2011), we transformed wild-type or *nhx1*Δ BJ3505 cells with pCB046, a yeast expression vector containing a genetically encoded pH probe (pHlourin fused to mCherry) fused to the C-terminus of Pep12 to exclusively target it to the lumen of MVBs. To generate the calibration curves shown in Figure 3E, 12 µg of organelles was added to 60 µl reaction buffer containing 50 µM nigericin in PS buffer titrated to pH values between 5.8 and 8.0 and incubated at 27°C for 10 min. Fluorescence intensities for pHluorin (excitation at 485 nm, emission at 520 nm) and mCherry (excitation at 584 nm, emission at 610 nm) were then measured with a Synergy H1 plate-reader, a multimode spectrophotometer (Biotek, Winooski, VT). A blank reference well containing 60 µl PS was used to detect background fluorescence. Ratios of background-subtracted pHluorin:mCherry fluorescence values were then plotted versus pH. Fluorescence values obtained under standard fusion conditions (Figure 3F) were then compared with this curve to estimate MVB pH in vitro. Experimental results shown are the best representatives of three biological replicates, each repeated twice (six technical replicates total).

Fluorescence microscopy

Live yeast cells were stained with FM4-64 to label vacuole membranes using a pulse-chase method as previously described (Brett *et al.,* 2008). Membranes of isolated organelles were stained by adding 3 µM FM4-64 and incubating at 27°C for 10 min. Stained organelles were then added to standard fusion reaction buffer, incubated at 27°C for up to 60 min, and placed on ice prior to visualization. To obtain fluorescence micrographs, we used a Nikon Eclipse TiE inverted microscope equipped with a motorized laser TIRF illumination unit, Photometrics Evolve 512 electron multiplication charge-coupled device camera, an ApoTIRF 1.49 NA 100× objective lens, and bright (50 mW) blue and green solid-state lasers operated with Nikon Elements software (housed in the Centre for Microscopy and Cellular Imaging at Concordia University). Micrographs were processed using ImageJ software (National Institutes of Health), and Adobe Photoshop CC. Images shown were adjusted for brightness and contrast, inverted, and sharpened with an unsharp masking filter. Micrographs shown are the best representatives of at least three biological replicates, imaged at least six times each (a total of ≥18 technical replicates), whereby each field examined contained ≥35 cells or isolated organelles.

Data analysis and presentation

All quantitative data were processed using Microsoft Excel v.14.0.2 software (Microsoft Cooperation, Redmond, WA), including

calculation of means, SEMs and Student's two-tailed *t* tests. The *p* values <0.05 are indicated. Fusion values shown were normalized to values obtained under control conditions (organelles isolated from wild-type cells; pH 6.80; 125 mM KCl; ATP; no inhibitors, chloroquine, or GTPγS) where indicated. Data were plotted using Kaleida Graph v.4.0 software (Synergy Software, Reading, PA). All figures were prepared using Adobe Illustrator CC software (Adobe Systems, San Jose, CA). References were prepared using Mendeley software (Mendeley, New York, NY).

ACKNOWLEDGMENTS

We thank A. J. Merz and W. T. Wickner for antibodies. This work was supported by Natural Sciences and Engineering Research Council of Canada grants RGPIN/403537-2011 and RGPIN/2017-06652 awarded to C.L.B.

REFERENCES

Ali R, Brett CL, Mukherjee S, Rao R (2004). Inhibition of sodium/proton exchange by a Rab-GTPase-activating protein regulates endosomal traffic in yeast. J Biol Chem 279, 4498–4506.

Auffarth K, Arlt H, Lachmann J, Cabrera M, Ungermann C (2014). Tracking of the dynamic localization of the Rab-specific HOPS subunits reveal their distinct interaction with Ypt7 and vacuoles. Cell Logist 4, e29191.

Balderhaar HJ, Arlt H, Ostrowicz C, Brocker C, Sundermann F, Brandt R, Babst M, Ungermann C (2010). The Rab GTPase Ypt7 is linked to retromer-mediated receptor recycling and fusion at the yeast late endosome. J Cell Sci 123, 4085–4094.

Balderhaar HJ, Lachmann J, Yavavli E, Brocker C, Lurick A, Ungermann C (2013). The CORVET complex promotes tethering and fusion of Rab5/Vps21-positive membranes. Proc Natl Acad Sci USA 110, 3823–3828.

Bensen ES, Yeung BG, Payne GS (2001). Ric1p and the Ypt6p GTPase function in a common pathway required for localization of trans-Golgi network membrane proteins. Mol Biol Cell 12, 13–26.

Bowers K, Levi BP, Patel FI, Stevens TH (2000). The sodium/proton exchanger Nhx1p is required for endosomal protein trafficking in the yeast *Saccharomyces cerevisiae*. Mol Biol Cell 11, 4277–4294.

Brett CL, Donowitz M, Rao R (2005a). Evolutionary origins of eukaryotic sodium/proton exchangers. Am J Physiol Cell Physiol 288, C223–239.

Brett CL, Merz AJ (2008). Osmotic regulation of Rab-mediated organelle docking. Curr Biol 18, 1072–1077.

Brett CL, Plemel RL, Lobingier BT, Vignali M, Fields S, Merz AJ (2008). Efficient termination of vacuolar Rab GTPase signaling requires coordinated action by a GAP and a protein kinase. J Cell Biol 182, 1141–1151.

Brett CL, Tukaye DN, Mukherjee S, Rao R (2005b). The yeast endosomal $Na^+(K^+)/H^+$ exchanger Nhx1 regulates cellular pH to control vesicle trafficking. Mol Biol Cell 16, 1396–1405.

Brett CL, Wei Y, Donowitz M, Rao R (2002). Human Na^+/H^+ exchanger isoform 6 is found in recycling endosomes of cells, not in mitochondria. Am J Physiol Cell Physiol 282, C1031–1041.

Brunet S, Saint-Dic D, Milev MP, Nilsson T, Sacher M (2016). The TRAPP subunit Trs130p interacts with the GAP Gyp6p to mediate Ypt6p dynamics at the late Golgi. Front Cell Dev Biol 4, 48.

Cang C, Aranda K, Seo YJ, Gasnier B, Ren D (2015). TMEM175 is an organelle K^+ channel regulating lysosomal function. Cell 162, 1101–1112.

Cao Q, Zhong XZ, Zou Y, Murrell-Lagnado R, Zhu MX, Dong XP (2015). Calcium release through P2X4 activates calmodulin to promote endolysosomal membrane fusion. J Cell Biol 209, 879–894.

Cardon M, Evankovich KD, Holder JL Jr (2016). Exonic deletion of SLC9A9 in autism with epilepsy. Neurol Genet 2, e62.

Coonrod EM, Graham LA, Carpp LN, Carr TM, Stirrat L, Bowers K, Bryant NJ, Stevens TH (2013). Homotypic vacuole fusion in yeast requires organelle acidification and not the V-ATPase membrane domain. Dev Cell 27, 462–468.

Deane EC, Ilie AE, Sizdahkhani S, Das Gupta M, Orlowski J, McKinney RA (2013). Enhanced recruitment of endosomal Na^+/H^+ exchanger NHE6 into dendritic spines of hippocampal pyramidal neurons during NMDA receptor-dependent long-term potentiation. J Neurosci 33, 595–610.

Desfougères Y, Vavassori S, Rompf M, Gerasimaite R, Mayer A (2016). Organelle acidification negatively regulates vacuole membrane fusion *in vivo*. Sci Rep 6, 29045.

Eitzen G, Will E, Gallwitz D, Haas A, Wickner W (2000). Sequential action of two GTPases to promote vacuole docking and fusion. EMBO J 19, 6713–6720.

Epp N, Rethmeier R, Kramer L, Ungermann C (2011). Membrane dynamics and fusion at late endosomes and vacuoles—Rab regulation, multisubunit tethering complexes and SNAREs. Eur J Cell Biol 90, 779–785.

Fratti RA, Jun Y, Merz AJ, Margolis N, Wickner W (2004). Interdependent assembly of specific regulatory lipids and membrane fusion proteins into the vertex ring domain of docked vacuoles. J Cell Biol 167, 1087–1098.

Fratti RA, Wickner W (2007). Distinct targeting and fusion functions of the PX and SNARE domains of yeast vacuolar Vam7p. J Biol Chem 282, 13133–13138.

Gilfillan GD, Selmer KK, Roxrud I, Smith R, Kyllerman M, Eiklid K, Kroken M, Mattingsdal M, Egeland T, Stenmark H, *et al*. (2008). SLC9A6 mutations cause X-linked mental retardation, microcephaly, epilepsy, and ataxia, a phenotype mimicking Angelman syndrome. Am J Hum Genet 82, 1003–1010.

Gillooly DJ, Morrow IC, Lindsay M, Gould R, Bryant NJ, Gaullier JM, Parton RG, Stenmark H (2000). Localization of phosphatidylinositol 3-phosphate in yeast and mammalian cells. EMBO J 19, 4577–4588.

He J, Vora M, Haney RM, Filonov GS, Musselman CA, Burd CG, Kutateladze AG, Verkhusha VV, Stahelin RV, Kutateladze TG (2009). Membrane insertion of the FYVE domain is modulated by pH. Proteins 76, 852–860.

Henne WM, Buchkovich NJ, Emr SD (2011). The ESCRT pathway. Dev Cell 21, 77–91.

Heuser J (1989). Changes in lysosome shape and distribution correlated with changes in cytoplasmic pH. J Cell Biol 108, 855–864.

Hill JK, Brett CL, Chyou A, Kallay LM, Sakaguchi M, Rao R, Gillespie PG (2006). Vestibular hair bundles control pH with $Na^+(K^+)/H^+$ exchangers NHE6 and NHE9. J Neurosci 26, 9944–9955.

Huh WK, Falvo JV, Gerke LC, Carroll AS, Howson RW, Weissman JS, O'Shea EK (2003). Global analysis of protein localization in budding yeast. Nature 425, 686–691.

Jun Y, Wickner W (2007). Assays of vacuole fusion resolve the stages of docking, lipid mixing, and content mixing. Proc Natl Acad Sci USA 104, 13010–13015.

Kallay LM, Brett CL, Tukaye DN, Wemmer MA, Chyou A, Odorizzi G, Rao R (2011). Endosomal $Na^+(K^+)/H^+$ exchanger Nhx1/Vps44 functions independently and downstream of multivesicular body formation. J Biol Chem 286, 44067–44077.

Karim MA, Mattie S, Brett CL (2017). Distinct features of multivesicular body-lysosome fusion revealed by a new cell-free content-mixing assay. bioRxiv 133074; doi: https://doi.org/10.1101/133074.

Kojima A, Toshima JY, Kanno C, Kawata C, Toshima J (2012). Localization and functional requirement of yeast Na^+/H^+ exchanger, Nhx1p, in the endocytic and protein recycling pathway. Biochim Biophys Acta 1823, 534–543.

Kondapalli KC, Hack A, Schushan M, Landau M, Ben-Tal N, Rao R (2013). Functional evaluation of autism-associated mutations in NHE9. Nat Commun 4, 2510.

Kondapalli KC, Llongueras JP, Capilla-González V, Prasad H, Hack A, Smith C, Guerrero-Cázares H, Quiñones-Hinojosa A, Rao R (2015). A leak pathway for luminal protons in endosomes drives oncogenic signalling in glioblastoma. Nat Commun 6, 6289.

Kümmel D, Ungermann C (2014). Principles of membrane tethering and fusion in endosome and lysosome biogenesis. Curr Opin Cell Biol 29, 61–66.

Lasky-Su J, Neale BM, Franke B, Anney RJ, Zhou K, Maller JB, Vasquez AA, Chen W, Asherson P, Buitelaar J, *et al*. (2008). Genome-wide association scan of quantitative traits for attention deficit hyperactivity disorder identifies novel associations and confirms candidate gene associations. Am J Med Genet B Neuropsychiatr Genet 147B, 1345–1354.

Lawrence G, Brown CC, Flood BA, Karunakaran S, Cabrera M, Nordmann M, Ungermann C, Fratti RA (2014). Dynamic association of the PI3P-interacting Mon1-Ccz1 GEF with vacuoles is controlled through its phosphorylation by the type 1 casein kinase Yck3. Mol Biol Cell 25, 1608–1619.

Lim CY, Zoncu R (2016). The lysosome as a command-and-control center for cellular metabolism. J Cell Biol 214, 653–664.

Longtine MS, McKenzie A, Demarini DJ, Shah NG, Wach A, Brachat A, Philippsen P, Pringle JR (1998). Additional modules for versatile and economical PCR-based gene deletion and modification in *Saccharomyces cerevisiae*. Yeast 14, 953–961.

Luo Z, Gallwitz D (2003). Biochemical and genetic evidence for the involvement of yeast Ypt6-GTPase in protein retrieval to different Golgi compartments. J Biol Chem 278, 791–799.
Luzio JP, Gray SR, Bright N (2010). Endosome-lysosome fusion. Biochem Soc Trans 38, 1413–1416.
Markunas CA, Quinn KS, Collins AL, Garrett ME, Lachiewicz AM, Sommer JL, Morrissey-Kane E, Kollins SH, Anastopoulos AD, Ashley-Koch AE (2010). Genetic variants in SLC9A9 are associated with measures of attention-deficit/hyperactivity disorder symptoms in families. Psychiatr Genet 20, 73–81.
Maxson ME, Grinstein S (2014). The vacuolar-type H^+-ATPase at a glance—more than a proton pump. J Cell Sci 127, 4987–4993.
Mitsui K, Koshimura Y, Yoshikawa Y, Matsushita M, Kanazawa H (2011). The endosomal Na^+/H^+ exchanger contributes to multivesicular body formation by regulating the recruitment of ESCRT-0 Vps27p to the endosomal membrane. J Biol Chem 286, 37625–37638.
Morrow EM, Yoo SY, Flavell SW, Kim TK, Lin Y, Hill RS, Mukaddes NM, Balkhy S, Gascon G, Hashmi A*, et al.* (2008). Identifying autism loci and genes by tracing recent shared ancestry. Science 321, 218–223.
Nass R, Cunningham KW, Rao R (1997). Intracellular sequestration of sodium by a novel Na^+/H^+ exchanger in yeast is enhanced by mutations in the plasma membrane H^+-ATPase. Insights into mechanisms of sodium tolerance. J Biol Chem 272, 26145–26152.
Nass R, Rao R (1998). Novel localization of a Na^+/H^+ exchanger in a late endosomal compartment of yeast. Implications for vacuole biogenesis. J Biol Chem 273, 21054–21060.
Nickerson DP, Brett CL, Merz AJ (2009). Vps-C complexes: gatekeepers of endolysosomal traffic. Curr Opin Cell Biol 21, 543–551.
Ouyang Q, Lizarraga SB, Schmidt M, Yang U, Gong J, Ellisor D, Kauer JA, Morrow EM (2013). Christianson syndrome protein NHE6 modulates TrkB endosomal signaling required for neuronal circuit development. Neuron 80, 97–112.
Pearce DA, Ferea T, Nosel SA, Das B, Sherman F (1999). Action of BTN1, the yeast orthologue of the gene mutated in Batten disease. Nat Genet 22, 55–58.
Peters C, Bayer MJ, Bühler S, Andersen JS, Mann M, Mayer A (2001). *Trans*-complex formation by proteolipid channels in the terminal phase of membrane fusion. Nature 409, 581–588.
Peterson MR, Burd CG, Emr SD (1999). Vac1p coordinates Rab and phosphatidylinositol 3-kinase signaling in Vps45p-dependent vesicle docking/fusion at the endosome. Curr Biol 9, 159–162.
Prasad H, Rao R (2015). The Na^+/H^+ exchanger NHE6 modulates endosomal pH to control processing of amyloid precursor protein in a cell culture model of Alzheimer disease. J Biol Chem 290, 5311–5327.
Qiu QS, Fratti RA (2010). The Na^+/H^+ exchanger Nhx1p regulates the initiation of *Saccharomyces cerevisiae* vacuole fusion. J Cell Sci 123, 3266–3275.
Robinson JS, Klionsky DJ, Banta LM, Emr SD (1988). Protein sorting in *Saccharomyces cerevisiae*: isolation of mutants defective in the delivery and processing of multiple vacuolar hydrolases. Mol Cell Biol 8, 4936–4948.
Rothman JH, Howald I, Stevens TH (1989). Characterization of genes required for protein sorting and vacuolar function in the yeast *Saccharomyces cerevisiae*. EMBO J 8, 2057–2065.
Russell MRG, Shideler T, Nickerson DP, West M, Odorizzi G (2012). Class E compartments form in response to ESCRT dysfunction in yeast due to hyperactivity of the Vps21 Rab GTPase. J Cell Sci 125, 5208–5220.
Schwartz ML, Merz AJ (2009). Capture and release of partially zipped trans-SNARE complexes on intact organelles. J Cell Biol 185, 535–549.
Shin JJ, Loewen CJ (2011). Putting the pH into phosphatidic acid signaling. BMC Biol 9, 85.
Starai VJ, Thorngren N, Fratti RA, Wickner W (2005). Ion regulation of homotypic vacuole fusion in S*accharomyces cerevisiae*. J Biol Chem 280, 16754–16762.
Strasser B, Iwaszkiewicz J, Michielin O, Mayer A (2011). The V-ATPase proteolipid cylinder promotes the lipid-mixing stage of SNARE-dependent fusion of yeast vacuoles. EMBO J 30, 4126–4141.
Strom M, Vollmer P, Tan TJ, Gallwitz D (1993). A yeast GTPase-activating protein that interacts specifically with a member of the Ypt/Rab family. Nature 361, 736–739.
Strømme P, Dobrenis K, Sillitoe RV, Gulinello M, Ali NF, Davidson C, Micsenyi MC, Stephney G, Ellevog L, Klungland A, Walkley SU (2011). X-linked Angelman-like syndrome caused by Slc9a6 knockout in mice exhibits evidence of endosomal-lysosomal dysfunction. Brain 134, 3369–3383.
Stroupe C, Collins KM, Fratti RA, Wickner W (2006). Purification of active HOPS complex reveals its affinities for phosphoinositides and the SNARE Vam7p. EMBO J 25, 1579–1589.
Suda Y, Kurokawa K, Hirata R, Nakano A (2013). Rab GAP cascade regulates dynamics of Ypt6 in the Golgi traffic. Proc Natl Acad Sci USA 110, 18976–18981.
Tall GG, Hama H, DeWald DB, Horazdovsky BF (1999). The phosphatidylinositol 3-phosphate binding protein Vac1p interacts with a Rab GTPase and a Sec1p homologue to facilitate vesicle-mediated vacuolar protein sorting. Mol Biol Cell 10, 1873–1889.
Thorngren N, Collins KM, Fratti RA, Wickner W, Merz AJ (2004). A soluble SNARE drives rapid docking, bypassing ATP and Sec17/18p for vacuole fusion. EMBO J 23, 2765–2776.
Vollmer P, Will E, Scheglmann D, Strom M, Gallwitz D (1999). Primary structure and biochemical characterization of yeast GTPase-activating proteins with substrate preference for the transport GTPase Ypt7p. Eur J Biochem 260, 284–290.
Wickner W (2010). Membrane fusion: five lipids, four SNAREs, three chaperones, two nucleotides, and a Rab, all dancing in a ring on yeast vacuoles. Annu Rev Cell Dev Biol 26, 115–136.
Will E, Gallwitz D (2001). Biochemical characterization of Gyp6p, a Ypt/Rab-specific GTPase-activating protein from yeast. J Biol Chem 276, 12135–12139.
Yang L, Faraone SV, Zhang-James Y (2016). Autism spectrum disorder traits in Slc9a9 knock-out mice. Am J Med Genet B Neuropsychiatr Genet 171B, 363–376.